

## Prediction of Methyl Orange (MO) Toxicity and Minimizing Its Pollution in Aquatic Environment by Activated Carbon Adsorption

<sup>1</sup>Salwan Sufyan Ibrahim, <sup>1</sup>Safauldeen Adnan, <sup>1</sup>Ammar Salim Manati, <sup>2</sup>Kafa Khalaf Hammud\*

<sup>1</sup>Ministry of Science and Technology – Iraq

<sup>2</sup>Iraqi Atomic Energy Commission – Iraq

### Article information

#### Article history:

Received: May, 27, 2023

Accepted: August, 04, 2023

Available online: December, 14, 2023

#### Keywords:

Prediction,

Pollution,

Activated carbon,

Face tissue

#### \*Corresponding Author:

Kafa Khalaf Hammud

[kafaakhalaf@gmail.com](mailto:kafaakhalaf@gmail.com)

#### DOI:

<https://doi.org/10.53523/ijoirVolXIXIDxx>

This article is licensed under:

[Creative Commons Attribution 4.0 International License](https://creativecommons.org/licenses/by/4.0/).

### Abstract

Minimizing environmental pollution is an essential work of the official and scientific communities around the world, especially in water systems. In water, soluble dye works as a blockage in photosynthesis process because of its toxicity. One of these highly applicable dyes in industry is Methyl Orange (MO), documented with more than 10% released to water. Here, a new Iraqi try of converting environmental and health problems to solutions with high quantification was as done by using face tissue (Kleenex) as a carbon source. Primary *in Silico* testing of this anionic dye (Methyl Orange) was done based on online website confirmed MO dye is unsafe in several toxicological determinations such as foetus health (during pregnancy). Also, it is permeable material to skin, Blood- Brain system (BBB), and Human Colon Carcinoma cell line (CaCO<sub>2</sub>) compatible with Human Intestinal absorption (74.166%). In experimental section, low quality of face tissue (Kleenex) was subject to a high acidic medium (concentrated sulphuric acid), followed by addition of sodium carbonate to .increase activation of based carbon material with more structural pores yielding high removal efficiency and adsorption capacity ranged (88-98)% and (88-98) mg/g respectively. Qualitative and quantitative evaluations were based upon choosing two wavelengths in ultraviolet (272 nm) and visible (464 nm) regions. In this work, two removal steps were performed with the same adsorbent companied by multiple UV-Vis spectroscopic evaluation of several tested sections. Reviewing of published papers in MO removal presents the extraordinary performance of this prepared material towards using it as an excellent adsorbent of toxic material in aqueous solution.

### 1. Introduction

Methyl Orange (MO) is a known titration indicator in analytical chemistry where its 1% aqueous solution gives red and yellow at acidic pH 3.1 and 4.4 respectively. This sodium p-dimethyl amino azobenzene sulfonate (C.I. 13025, Gold Orange, Acid Orange 52; Orange III, C<sub>14</sub>H<sub>14</sub>N<sub>3</sub>NaO<sub>3</sub>S) is widely used in the textile industry. Water soluble - dyes forms a coloured system working as a blockage in photosynthesis process that occurred and needed to aqua creatures [1-3].

Methyl Orange (MO) has high water solubility and is a toxic material to all species in the environment resulted from more than 10% released to water. Removal of dyes is a necessary step for life progress especially into the water environment. In general, removal techniques are varied between chemical, physical, and biological degradation methods. Various adsorption studies were concluded in dye subject and in particular MO issues by applying simple – efficient and low – cost material such as chitosan hydrogel beds, clay, rice husk, activated carbon, bacterial or fungal sorbent, industrial by-products, agricultural wastes, and human wastes [1-13].

Computer –assistance methods in biological studies are focusing on finding how much clinical outcomes are true. They are very helpful in finding molecular actions outside lab complications and cost besides limits of using animal experiments. These machine learning methods (*in Silico*) open a wide window for potential therapeutics starting from molecular structure. This superior window provide an excellent look to unknown or recognized molecular structures for future area in genetic engineering, cancer, vaccine, and other biotechnology zones [14 - 17].

This paper targets human safety by looking in two scientific paths. The first path involves *in Silico* prediction of Absorption, Distribution, Metabolism, Excretion and Toxicity (ADMET) linked to this orally acute toxic material. The second path provides experiments in pollution minimizing by activated carbon depending on facial tissues. Face tissues (named in Iraq as Kleenex) are widely used material especially in Covid-19 period, which represented a critical health problem in dealing with their waste. So, choosing face tissues as a carbon based material with chemical modification may became a solution from environment and health problems.

Here, an online website coded as <https://biosig.lab.uq.edu.au/tools> was chosen in looking for MO pharmacokinetic and toxicity characterizations by means of graph-based signature. Low cost material (face tissue) was subjected for removal of MO after conversion step to activated carbon with concentrated sulphuric acid and sodium carbonate. Also, efficiency of repeating removal step with the same adsorbent was another goal through UV-Vis spectroscopic evaluation of the first and last 5 mL, and the total eluted MO solution. Mathematical evaluation of the removal efficiency and adsorption capacity of the prepared activated (5 grams) by passing one litre (500 ppm) was done.

## 2. Experimental Procedure

**Chemicals:** Sulphuric acid and sodium carbonate were purchased from BDH and Merck companies.

**Instruments:** Qualitative and quantitative analyses were done by UV-VIS spectrophotometer (Shimadzu, Japan).

**Methods:** *In Silico* – ADMET prediction: various online ADMET websites were applied to determine Methyl Orange characters basing upon Simplified Molecular-Input Line-Entry System (SMILES) specification: CN(C)C1=CC=C(C=C1)N=NC2=CC=C(C=C2)S(=O)(=O)[O-].[Na+] including water solubility, Human Intestinal absorption, Embryo-toxicity, BBB and CNS permeability, Hepatotoxicity, skin sensitization, substrate evaluation and inhibition of Cytochrome P450 Family, and others through [18, 19, 20]. Collected results were tabulated as in Tables (1 & 2).

**Preparation of the adsorbent:** Low - quality face tissues known in Iraqi society as Kleenex was purchased from the local Baghdad market. (56.4320, 58.6100) grams of this cellulose ((C<sub>6</sub>H<sub>10</sub>O<sub>5</sub>)<sub>n</sub>) source were soaked in 150 mL of concentrated sulphuric acid for several days until all tissues turned to black colour. One gram of sodium carbonate was added to the mixture as an additional activation step. The resultant activated carbon was washed with deionized water until pH7 then dried at 70°C. The conversion quantity of the produced activated carbon was more than 30% (Table 3).

**Table (1).** Molecular, predicted ADMET descriptions of Methyl Orange.

logP	Hydrogen bonding acceptor – donor	Surface area	Water solubility (logmol/L)
0.0761	6 - 0	151.467	-2.31
Caco2 permeability (g Papp in 10 <sup>-6</sup> cm/s)	Human Intestinal absorption (% adsorbed)	Skin Permeability (log Kp)	Embryo-toxicity
0.889	74.166	2.735	Unsafe
BBB permeability (logBB)	CNS permeability (log PS)	Total Clearance (log ml/min/kg)	Human Max. tolerated dose (log mg/kg/day)
0.811	-2.784	0.787	0.623
CYP2D6 and CYP3A4 substrate	CYP1A2, CYP2C19, CYP2C9, CYP2D6, and CYP3A4 inhibitor	P-glycoprotein substrate, inhibitor I, II	Renal OCT2 substrate
No	No	No	No
Ames	hERG I & II inhibitor	Hepatotoxicity	Skin sensitization
No	No	No	No
Oral Rat Acute Toxicity (LD50, mol/kg)	Oral Rat Chronic Toxicity (LOAEL, log mg/kg_bw/day)	<i>T.Pyriformis</i> toxicity (log ug/L)	Minnow toxicity (log mM)
1.781	1.962	0.284	0.34

**Table (2).** Methyl orange prediction with related environmental toxicities.

Website reference	Honey bee	Avian	Ames
[19]	No	No	No
	Minnow	Rat acute (LD <sub>50</sub> )	Oral Rat Chronic Toxicity (LOAEL)
	1.905	886.4	6.3
[20]	Breast	CNS	Colon
	4.255 – 4.892	4.108 – 4.665	4.153 – 4.853
	Leukaemia	Melanoma	Ovarian
	4.383 – 4.871	4.218 – 4.453	4.23 – 4.523
	Prostate	Renal	Lung
	4.231 -4.818	4.18 -4.609	Non small: 4.238 -4.612 Small: 4.245 – 4.323

**Table (3).** Conversion of face tissues to activated carbon.

Initial weight of face tissue, grams	Final weight of the produced activated carbon after drying, grams	Conversion quantity, %
56.4320	18.5200	32.8183
58.6100	20.3100	34.6528

Standard Solutions and trend line characters: Methyl Orange solutions (CAS registry number: 547-58-0) with concentration range (1-100) ppm were prepared for standard curve qualification and quantification. For estimation of calibration curve equation and linear regression ( $R^2$ ), two wavelength peaks (272 and 464) nm were evaluated (Figures 1).

Linearity of the standard curve at each wavelength was the controller of choosing concentration range towards calculating trending line (equation and  $R^2$ ) (Figure 2). At 464 nm,  $R^2$  trended to less value (0.8371) when the standard solution range was (1-100) ppm compared to (0.9934) with range (1-40) ppm. This important note determined trend line equation then calculating the resulted solution after adsorption step. From trend lines in Figure (2), molar absorptivity, Lambert – Beer range, intercept, linear regression ( $R^2$ ), and trend line equation for both wavelengths (272 and 464) nm are tabulated (Table 4).

**Table (4).** Linear equation data at (272 and 464) nm.

	272 nm	464 nm
<b>Lambert – Beer range</b>		
<b>ppm</b>	1-100	1-40
<b>Mole/L</b>	$3.05493 \times 10^{-6}$ - $3.05493 \times 10^{-4}$	$3.05493 \times 10^{-6}$ - $1.22197 \times 10^{-4}$
<b>Trend line equation</b>	$y = 8408.7x + 0.0123$	$y = 19652x + 0.0826$
<b>Linear regression (<math>R^2</math>)</b>	0.9999	0.9934
<b>Molar absorptivity,</b>		
<b>L mol.<sup>-1</sup> cm<sup>-1</sup></b>	8408.7	19652

Adsorption steps: At room temperature, Methyl Orange solution (500 ppm, 1L) was adsorbed by the prepared activated carbon (5grams). Collected samples after adsorption stage were first collected 5 mL, final collected 5 mL, and whole collected sample where the adsorbent was in filter paper located in a simple funnel. After complete the first adsorption step of whole 1L of this azo dye, another 1L was added to the same adsorbent and the same collections (first, last, mixture) were evaluated by UV-Vis instrument.

Removal efficiency (R%) and adsorption capacity (Q, mg/g) were calculated and tabulated (Table 5) where:

$$\text{Removal efficiency (R\%)} = [(C_0 - C_i) / C_0] \times 100 \dots\dots (1)$$

$$\text{Adsorption capacity (Q)} = [(C_0 - C_i) / m] \times (V) \dots\dots (2)$$

where  $C_0$  = initial concentration, ppm;  $C_i$  = concentration at specific step, ppm;  $m$  = mass of the adsorbent, gram;  $V$  = solution volume, Litre.

**Table (5).** Adsorption results of Methyl Orange by using face tissue activated carbon.

Identity	Concentration, ppm		Removal efficiency (R%)		Adsorption capacity (Q), mg/g	
	272 nm	464 nm	272 nm	464 nm	272 nm	464 nm
<b>First 5mL</b>	44.92996	16.70667	91.01401	96.65867	91.01401	96.65867
<b>Final 5 mL</b>	58.27626	42.35667	88.34475	91.52867	88.34475	91.52867
<b>Total mixture</b>	47.57588	28.59000	90.48482	94.282	90.48482	94.282
<b>First 5mL, 2<sup>nd</sup> repeat</b>	22.47860	9.173333	95.50428	98.16533	95.50428	98.16533
<b>Final 5mL, 2<sup>nd</sup> repeat</b>	21.79	27.96498	95.642	94.407	95.642	94.407
<b>Total mixture</b>	48.08171	-	90.38366	-	90.38366	-

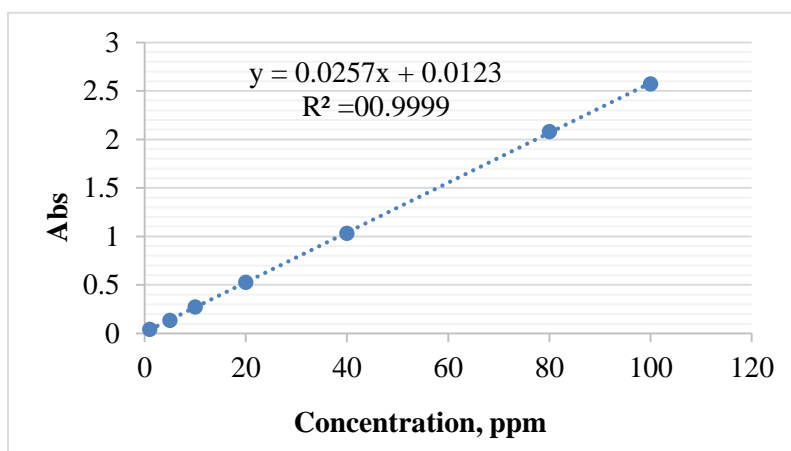


**Figure (1).** Standard curve of Methyl Orange solutions at 272 nm.

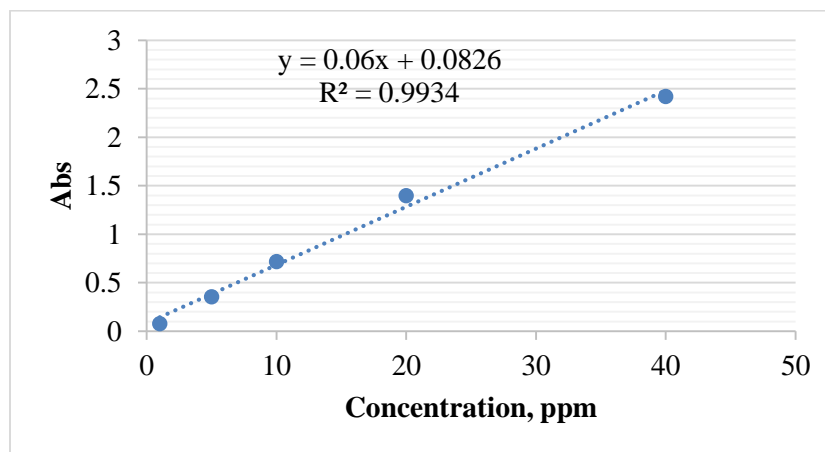


**Figure (2).** Standard curve of Methyl Orange solution at 464 nm.

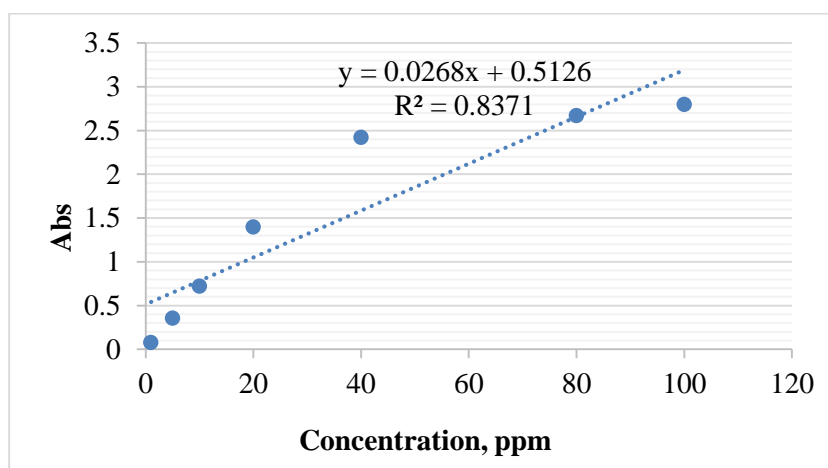


**Figure (3).** Standard solutions (1-100) ppm of Methyl Orange at 464 nm.

### 3. Results and Discussion

Here, a new *in Silico* evaluation of pollutant defined as the azo dye Methyl Orange (MO) that is widely applied in textile industry was done by placing [biosig] website as collective online website containing various docking and pharmacokinetic and toxicity prediction tools. In this paper, embryo, cancer, crop-, water solubility, Human Intestinal absorption, BBB and CNS permeability, Hepatotoxicity, skin sensitization, substrate evaluation and inhibition of Cytochrome P450 Family, and others are discussed. These characters were calculated with SMILES specification.

According to Tables (1 & 2), MO dye had a highly water solubility, surface area, and capability to form hydrogen bonding with aqua environments or cells. It is structurally unsafe to fetal health (during pregnancy) due to its permeability to skin, Caco2, Blood- Brain system (BBB) but not on liver, and Cytochrome P450 family under testing. Human Colon Carcinoma cell line (abbreviated as Caco-2) testing had  $0.889 \times 10^{-6}$  cm/s oral adsorption permeable rate for MO dye which was compatible with Human Intestinal absorption (74.166%).

Organic Cation Transporter 2 (OCT2) testing was with negative, meaning the renal system can clear MO and provide its elimination into the urine. Multidrug Resistance Protein (MDR1), a p-glycoprotein is a transporter that binds to Adenosine Triphosphate (ATP) and prevents cell uptake to chemicals, especially in cancer therapeutic issues. This p-glycoprotein reacts with any compound as a modulator, inducer, substrate or inhibitor [21].

Here, Methyl Orange showed (No) response to substrate or inhibitor I and II meaning p-glycoprotein is incapable of binding or transporting MO. Table (2) showed that MO is safe to honey bee, avian, and Ames testing. Also, prediction probabilities of breast, Central Nerve System (CNS), Colon, Leukaemia, Melanoma, Ovarian, Prostate, Renal, and Lung cell lines were less than 50%. These numeric probabilities are a good sign of a low concentration of MO.

Before proceeding with the discussion of our experimental steps, our working team tried using drip chamber for estimation the adsorption capacity and efficiency of Methyl Orange as a first Iraqi try. This anionic pollutant (500 ppm, 1L) was adsorbed with using an IV infusion set that is available in Iraqi market (Figure 4). Here, face tissue activated carbon (5 grams) was loaded then pressed with glass rod in the drip chamber of this medicinal set. This first try in Iraq and the other countries gave excellent results of adsorption (464 nm) as in Table (6), but the adsorption repeating caused inner pressure to prevent water with the remaining azo dye from passing. So, this technique was cancelled at the present time.

**Table (6).** Adsorption results of methyl Orange with using IV infusion chamber as a container of face tissue activated carbon.

Identity	Concentration, ppm	Removal efficiency (R%)	Adsorption capacity (Q), mg/g
First 5mL	3.031	99.3938	99.3938
Final 5 mL	10.586	97.8828	97.8828
Total mixture	39.941	92.0118	92.0118

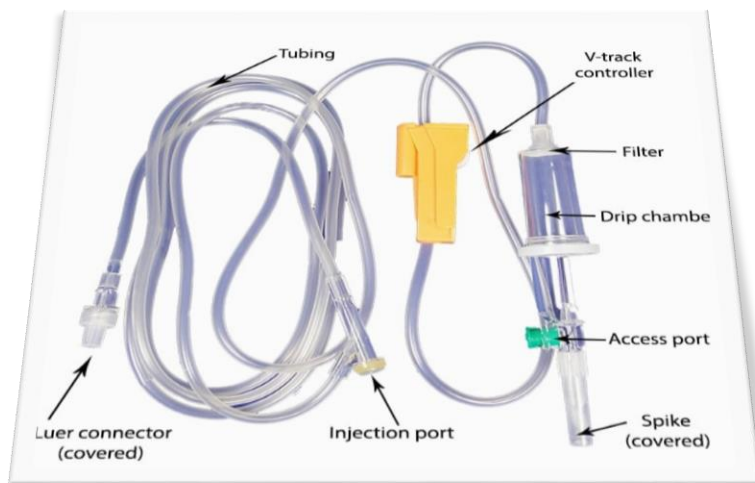


**Figure (4).** IV infusion set.

It is known that face tissue is a soft – disposable material made from available cellulose base material. This polysaccharide with general formula  $((C_6H_{10}O_5)_n)$  has more than 28% of carbon base if we considered that each unit contains six carbon atoms and five water molecules. So, the conversion percentage as in Table (3) confirmed a significant chemical transformation of face tissue (or Kleenex) to activated carbon by concentrated sulphuric acid and sodium carbonate. In general remark, the use of low quality of this face tissue (not waste) material was done for health consideration especially after Corona Virus pandemic.

In this work, two wavelengths (272 nm and 464 nm) were selected for removal efficiency and adsorption capacity of MO (Figure 5) that contains N=N, aromatic C=C, S=O, S-O, C-N, C-S, and C-C bonds having

$\sigma \rightarrow \sigma^*$ ,  $n \rightarrow \sigma^*$ ,  $\pi \rightarrow \pi^*$ , and  $n \rightarrow \pi^*$  transitions. Differences between these two absorption peaks are the keys in understanding the variations that represented in all calculated values (Table 7).

At low frequency, favoured  $\pi \rightarrow \pi^*$  transition of the anionic MO dye (solvate) has a strong interaction with solvent through hydrogen bonding with absence of the direct influence of azo (N=N) group in the region of high frequency. Presence of p- amino group may enhance basic property towards more hydrogen bonding interaction between solvent and solvate [22].

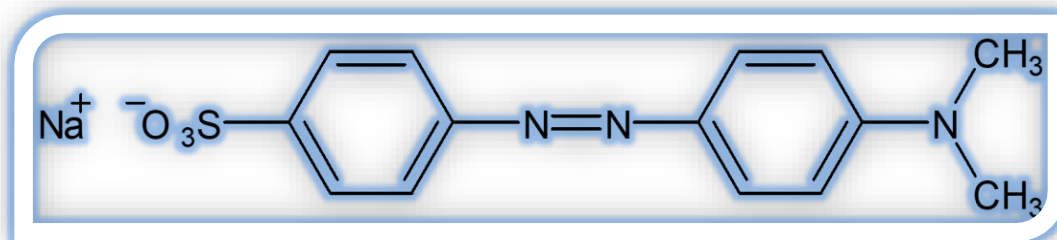


**Figure (5).** Chemical structure of Methyl Orange (MO).

Charge or electron transfer occurs in ultraviolet violet region and needs high energy to achieve this operation depending upon unsaturated and aromatic bonds while in visible region transition occurred with coloured species with less energy [23]. From Table (4), applying 272 nm gave wide MO concentration range, high  $R^2$  value, and low molar absorptivity compared to 464 nm calculation. These analytical notes may be associated to MO functional bonds that encouraged these foundations.

**Table (7).** Variation between 272 nm and 464 nm.

ID	272 nm	464 nm
Energy $\Delta E = hc/\lambda$ , kJ	$7.3014 \times 10^{-22}$	$4.2802 \times 10^{-22}$
Region	Ultraviolet (190-380) nm	Visible (380-780) nm

According to experimental section and related figures and tables, face tissue activated carbon showed excellent adsorption behavior with Methyl Orange dye from first collected 5 mL to all received solutions. Here, removal efficiency and adsorption capacity had the same numerical data at the same measured wavelength. The use of one liter and 5 grams in both calculated equations (Eq. 1 and Eq. 2) gave identical numbers of R% and Q. Table (5) shows maximum and minimum numerical data of the first try of adsorption steps compared to the first 5 mL of the second try (repeating step).

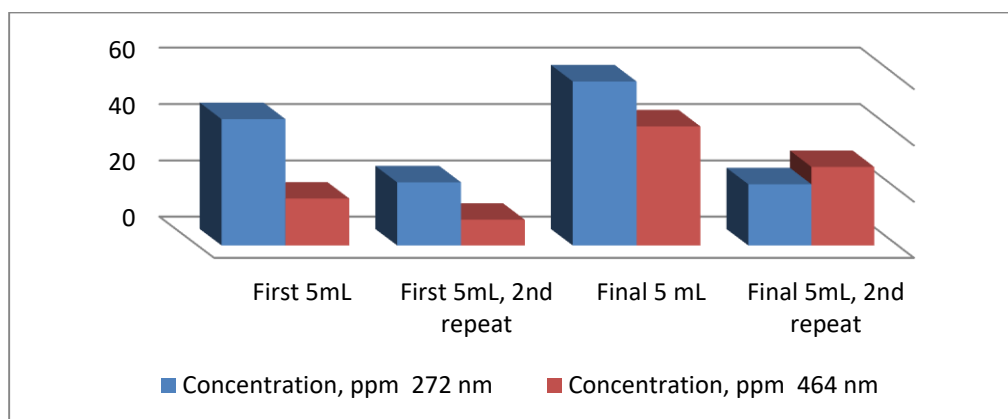
From Tables (5 & 8) and Figure (6), repeating step showed a significant removal of MO compared to the first adsorption step at both wavelengths. In the first step, each MO molecule is surrounding by water molecules as known solvation. Solvated MO occupies the pore of the prepared activated carbon and may be lost as a result of drying or gravity effects.

In the repeated step, dried (or non-solvated) MO with all charged and uncharged influences became an attracted center to the passed solvated MO in the pore. This expectation may be the only explanation of these changings in R% and Q calculations. So, repeating step becomes necessary to increase removal quantification which is a similar step in usual water filtration.



**Table (8).** Numerical comparison between first and second adsorption steps.

Identity	Concentration, ppm		Removal efficiency (R%)		Adsorption capacity (Q), mg/g	
	272 nm	464 nm	272 nm	464 nm	272 nm	464 nm
<b>First 5mL, 2<sup>nd</sup> repeat</b>	22.4786	9.17333	95.5043	98.1653	95.5043	98.1653
<b>Max.</b>	58.27626	42.35667	91.01401	96.65867	91.01401	96.65867
<b>Min.</b>	44.92996	16.70667	88.34475	91.52867	88.34475	91.52867

**Figure (6).** Comparison between first and second adsorption steps of Methyl Orange at (272 and 464) nm.

Removal efficiency and adsorption capacity in this work (Table 5) were high compared with scientific published papers (Table 9). Here, one liter was used in each step with 500 ppm through 5 g in a simple filtration technique, while published articles ranged from 100 to 500 mL. In conclusion, face tissue - activated carbon was excellent adsorbent for MO and may be used for continuing adsorption (or dye removal).

**Table (9).** Scientific published papers related to MO removal.

Source	Conditions	Results	Ref.
Populous leaves impregnated by acetic acid or L-arginine	Batch mode adsorption, agitation speed: 200 rpm, dosage: (0.2 g - 0.6 g)/100 mL MO, contact time (10 min - 100 min), pH (3–12), temperature (283.15–333.15) K, maximum absorption: 464 nm	L- Arginine, Langmuir capacity: 90.44 mg/g at pH 3, 303.15 K, $R^2 = 0.9988$ , pseudo-first order	12
Activated carbon sugarcane mud	pH 2, initial concentration: 24.17 ppm, dose: 0.5 g, contact time: 20 min.	removal 98.68%, adsorption capacity: 23.89 mg/g, Langmuir isotherm $R^2 = 0.9610$	8
Multi-walled carbon nanotubes (MWCNTs) membrane	diameters (12-15 nm, 30-50 nm), length (< 10 $\mu\text{m}$ ) pore size (0.032 nm), negative surface charge: -10.93 mV	Pure MWCNTs (30-50 nm) nanocomposite membrane: removal 86.77%, flux 0.82. diameter MWCNTs (12-15 nm): removal 83.37%, flux 0.76.	13
Cork powder	Batch experiments Temperature: 298 K, pH 2, dosage: 5.00 g l <sup>-1</sup> , particle size <0.08 mm, time: 10 hours	Adsorption capacity: 16.66 mg/ g $\Delta G^\circ$ : -14.96 kJ/ mole; $\Delta H^\circ$ : -11.71 kJ/ mole, $\Delta S^\circ$ : -10.93 J/ mole . K	7
Commercial coffee waste	Cationic surfactants cetyltrimethyl ammonium bromide or cetylpyridinium chloride Batch method	pH 3.5, 62.5 mg/g as max. adsorption capacity at 25 °C) 0.1 g/50 ml of adsorbent dose. pseudo-second-order kinetic Langmuir adsorption isotherm model	24
Polyaniline reinforced PANI@CA	Oxidation method	Surface area: near 332 m <sup>2</sup> g <sup>-1</sup> Total volume: 0.038 cm <sup>3</sup> g <sup>-1</sup> Removal capacity: 192.52 mg g <sup>-1</sup> at 298 K, pH 6 kinetic: pseudo second order rate chemisorption phase Langmuir model better match than the Freundlich model.	25

#### 4. Conclusion

A new Iraqi attempt at converting environmental and health problems into solutions with high quantification was as done by using face tissue (Kleenex) as a carbon source. Primary in Silico testing of this anionic dye (Methyl Orange) was done basing on an online website confirming toxicity in several toxicological determinations, such as fetal health (during pregnancy). Also, it is permeable material to skin, Blood- Brain system (BBB), and Human Colon Carcinoma cell line (Caco2) compatible with Human Intestinal absorption (74.166%). Prepared activated carbon adsorbed toxic MO dye with high removal efficiency and adsorption capacity. Qualitative and quantitative evaluations were based upon choosing two wavelengths in ultraviolet and visible regions. Reviewing of published papers in MO removal presents extraordinary performance of this prepared material towards using it as an excellent adsorbent of toxic material in aqueous solution.

**Conflict of Interest:** The authors declare that there are no conflicts of interest associated with this research project. We have no financial or personal relationships that could potentially bias our work or influence the interpretation of the results.

#### 5. References

- [1] T. Algarni and A. Al-Mohaimeed, "Water purification by adsorption of pigments or pollutants via metaloxide," *Journal of King Saud University – Science*, vol. 34, no. 8, article number 102339, 2022.
- [2] P. Boruah, P. Borthakur, and M. Das, "Magnetic metal / metal oxide nanoparticles and nanocomposite materials for water purification," *Nanoscale Materials in Water Purification*, Elsevier, USA, 2019.
- [3] S. Dutta, B. Gupta, S. Srivastava, and A. Gupta, "Recent advances on the removal of dyes from wastewater using various adsorbents: a critical review," *Materials Advances*, vol. 2, pp. 4497-4531, 2021.
- [4] J. Zhang, Q. Zhou, and L. Ou, "Kinetic, isotherm, and thermodynamic studies of the adsorption of methyl orange from aqueous solution by chitosan / alumina composite," *Journal of Chemical and Engineering Data* vol. 57, no. 2, pp. 412-419, 2012.
- [5] J. Zhong, "Photocatalytic decolorization of methyl orange solution with phosphotungstic acid," *Iranian Journal of Chemistry and Chemical Engineering* vol. 32, no. 1, pp. 57 – 65, 2013.
- [6] X. An, C. Gao, J. Liao, X. Wu, and X. Xie, "Synthesis of mesoporous N-doped TiO<sub>2</sub>/ZnAl-layered double oxides nanocomposite for efficient photodegradation of Methyl orange," *Materials Science Semiconductor Processing*, vol. 34, pp. 162–169, 2015.
- [7] F. Krika and O. Benlahbib, "Removal of methyl orange from aqueous solution via adsorption on cork as a natural and low-coast adsorbent: equilibrium, kinetic and thermodynamic study of removal process," *Desalination and Water Treatment* vol. 53, no. 13, pp. 3711 – 3723, 2015.
- [8] D. Rondina, D., Ymbong, M. Cadutdut, J. Nelasa, J. Paradero, V. Mabayo, and R. Arazo, " Utilization of a novel activated carbon adsorbent from press mud of sugarcane industry for the optimized removal of methyl orange dye in aqueous solution," *Applied Water Science* vol. 9, pp. 181, 2019.
- [9] S. Sativa, M. Zulfikar, A. Alni, "Optimization of pH and radiation time for photocatalytic activity of methyl orange using TiO<sub>2</sub>," *AIP Conference Proceedings* vol. 2331, article number 040006 (5 pages), 2021.
- [10] M. Hague, M. Haque, M. Mosharaf, and P. Marcus, "Decolorization degradation and detoxification of carcinogenic sulfonated azo dye methyl orange by newly developed biofilm consortia," *Saudi Journal of Biological Sciences* vol. 28, pp. 793-804, 2021.
- [11] L. Wu, X. Liu, G. Lv, R. Zhu, L. Tian, M. Liu, W. Rao, T. Liu, and L. Liao, "Study on the adsorption properties of methyl orange by natural one – dimensional nano- mineral materials with different structures," *Scientific Reports* vol. 11, article number 10640 (11 pages), 2021.
- [12] S. Shah, T. Sharma, B. Dar, and R. Bamezai, "Adsorptive removal of methyl orange dye from aqueous solution using populous leaves: Insights from kinetics, thermodynamics and computational studies", *Environmental Chemistry and Ecotoxicology*, vol. 3, pp. 172-181, 2021.
- [13] H. Chun, J. Lim, A., Idris, Y. Teow, and N. Ng, "Effect of Diameter of Carbon Nanotubes in Nanocomposite Membrane for Methyl Orange Dye Removal", *Journal of Applied Membrane Science and Technology*, vol. 27, no. 1, pp. 47–61, 2023.
- [14] M. Mehmood, U. Sehar, and N. Ahmad, "Use of Bioinformatics Tools in Different Spheres of Life Sciences", *Data Mining in Genomics and Proteomics* vol. 5, pp. 158, 2014.
- [15] A. Vellido, "The importance of interpretability and visualization in machine learning for applications in medicine and health care", *Neural Computing and Applications* vol. 2019, pp. 1–15, 2019.

- M. Sadeghi, M. Moradi, H. Madanchi, and B. Johari, "In silico study of garlic (*Allium sativum* L.)-derived compounds molecular interactions with  $\alpha$ -glucosidase", *In Silico Pharmacology* vol. 9, no. 1, pp. 11, 2021.
- [16] M. Moradi, R. Golmohammadi, A. Najafi, M. Moghaddam, M. Fasihi – Ramandi, and R. Mimejad, "A contemporary review on the important role of *in silico* approaches for managing different aspects of COVID-19 crisis", *Informatics in Medicine Unlocked*, Vol. 28, article number 100862, 2022.
- [17] D. Pires, T. Blundell, and D. Ascher, "pkCSM: Predicting Small-Molecule Pharmacokinetic and Toxicity Properties Using Graph-Based Signatures," *Journal of medicinal chemistry*, vol. 58, no. 9, pp.4066–4072, 2015.
- [18] D. Pires, K. Stubbs, J. Mylne, and D. Ascher, "cropCSM: designing safe and potent herbicides with graph based signatures," *Briefings in Bioinformatics*, vol. 23, no. 2, article number bbac042, 2022.
- [19] R. Al-Jarf, A. de Sa, D. Pires, and D. Ascher, "pdCSM-cancer: Using Graph-Based Signatures to Identify Small Molecules with Anticancer Properties," *Journal of Chemical Information and Modeling*, vol. 61, no. 7, pp.3314-3322, 2021.
- [20] A. Seelig, "p-Glycoprotein: one mechanism, many tasks and the consequences for pharmacotherapy of cancers", *Frontier on Oncology*, vol. 10, article number 576559, 2020.
- [21] R. Reeves and R. Kaiser, "Analysis of the visual spectrum of methyl orange in solvent and in hydrophobic binding sites," *Canadian Journal of Chemistry*, vol. 51, pp. 628 -635, 1973.
- [22] E. Sjulstok, G. Lüdemann, T. Kubař, M. Elstner, and I. Solov'yov, "Molecular Insights into Variable Electron Transfer in Amphibian Cryptochrome", *Biophysical Journal*, vol. 114, no. 11, pp. 2563-2572, 2018.
- [23] R. Lafi and A. Hafiane, " Removal of methyl orange (MO) from aqueous solution using cationic surfactants modified coffee waste (MCWs)", *Journal of the Taiwan Institute of Chemical Engineers*, vol. 58, pp. 424-433, 2016.
- [24] A. Bekhoukh, I. Moulefera, F. Zeggai, A. Benyoucef , and K. Bachari, " Anionic Methyl Orange Removal from Aqueous Solutions by Activated Carbon Reinforced Conducting Polyaniline as Adsorbent: Synthesis, Characterization, Adsorption Behavior, Regeneration and Kinetics Study", *Journal of Polymers and Environment*, vol. 30, pp. 886–895, 2022.